Acta. Chim. Asiana., 2025, 8(1), 299 – 605
e-ISSN/p-ISSN 2550-0503/2550-049x
Available online at: www.aca.unram.ac.id

RESEARCH PAPER

# Hydrothermal Synthesis of Crystalline Aluminium(III)-Tartrate: Effect of Tartrate Type and Molar Ratio

Yuniar Ponco Prananto,*[a] Danar Purwonugroho,[a] M. Naufal Tsaqif Dzakwan,[a] Tutik Setianingsih,[a] Nidatul Syarifah[a]

[a] Department of Chemistry, Universitas Brawijaya, Indonesia
Jl. Veteran No. 01 Malang, Indonesia

*E-mail: prananto@ub.ac.id

DOI: 10.29303/aca.v8i1.244

**Article info:**

Received 23/04/2025

Revised 28/05/2025

Accepted 29/05/2025

Available online 30/05/2025

**Abstract:** Aluminium(III)-tartrate (Al-T) complex is a compound that commonly used as mordent in textile dyeing. This complex is soluble in hot water; thus, information on the isolation of crystallised Al-T is limited. Isolation of crystallised Al-T is needed to gain a high purity complex for further application in the textile industry. This study aims to synthesize and isolate crystalline complex of Al-T. Hydrothermal method was used to obtain the targeted complex. Effects of tartrate precursor and Al(III):tartrate mol ratio in the synthesis of Al-T complex were also investigated. The synthesis was done at 150 °C for 24 hours in several Al(III):tartrate mol ratios (1:2, 2:1, and 2:3) using two different tartrate precursors, namely L-tartaric acid and KNa-tartrate. The synthesized complexes were identified by infrared spectroscopy and powder-XRD analyses, and then further characterised by UV Vis - DRS, DTA-TGA, and SEM. Experimental data shows that the mol ratio affects the precipitation of the Al-T complex, in which a white crystalline solid was only precipitated out from the 2:1 reaction by both tartrate precursors. Different tartrate precursors used in the synthesis may alter the crystallization and result in an Al-T complex with slightly different thermal decomposition profile, UV-Vis DRS spectra profile, and different yield due to the different nature of the tartrate precursor. This finding is expected to support the possibility of Al-T mass production as mordent in textile dyeing.

**Keywords:** metal complex, mordent, crystalline material, precursor, mol ratio.

**Citation:** Prananto, Y. P., Purwonugroho, D., Dzakwan, M. N. T., Setianingsih, T., & Syarifah, N. 2025. Synthesis of Microcrystalline Aluminium(III)-Tartrate by Hydrothermal Reaction: Effect of Tartrate Precursor and Mol Ratio. *Acta Chimica Asiana*, 8(1), 599–605. https://doi.org/10.29303/aca.v8i1.244

## INTRODUCTION

Aluminium is available in Indonesia, either from mineral ores, such as *bauxite*, clays, and muds, or from recycled aluminium products [1, 2, 3]. Aluminium can be converted into functional materials, one of which is a metal complex that is classified as metal-organic frameworks or MOF. The MOF can be further used in gas separation, heterogeneous catalysis, *etc* [4]. The production process of Al-MOF is considerably straightforward and can be done by solvothermal or hydrothermal methods. It can also be prepared at mild temperatures and using low-cost materials [3].

MOFs are coordination polymers made of metal ions and bridging units, which can be porous and have a high surface area [5]. MOF is a solid material with a three-dimensional structural framework and frequently has pores; thus, it is often used as a functional material such as an adsorbent, photocatalyst, etc [6]. MOF materials have several excellent characteristics, such as high porosity, large surface area, good structural adjustment, crystallinity and functional diversification, and can be utilised in vast applications [7]. MOF has been applied in various fields, such as for energy storage [8], fluorine removal from water [9], magnetic materials, gas adsorption, and luminescence materials [10], drug or biomolecule release agents [11], heterogeneous catalysis [12], and ionic conductivity [13, 14].

In general, complex of aluminium(III)-tartrate (Al-T), odorless white solid that is partly soluble in water, can be made by reacting Al(III) ions and tartrate ligands. Tartrate (Figure 1) is a polycarboxylate anionic ligand that easily binds to metal ions with various coordination modes. Previously, Al-T was prepared by direct mixing method from aluminium(III) chloride in a mixed solvent of water-ethanol at room temperature. The highest yield (97%) was obtained when the reaction used pH above 3 [15]. This work used hydrothermal method because it can hold the reaction at high temperatures and pressure with water as the solvent. Thus, it is expected to give a better chance to get the crystalline Al-T complex.

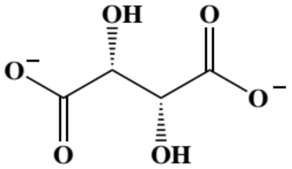

**Figure 1.** Structure of *L*-tartrate Ions

Al-T is reported to be massively used in textile dying as mordent [16] and in medical applications [17]. In general, inorganic tartrate salts from the main metal group have also been used as transducers due to their ferro-piezoelectricity and being developed for laser diodes [18]. Moreover, tartrate precursors are available in various commercial compounds and can be obtained at affordable prices. In addition, crystallization of tartrate complexes can be affected by reaction conditions (*i.e.* mol ratio, metal or ligand precursors, solvent, etc), in which small changes in reaction condition may alter the properties of the synthesized product [19].

This paper reports the hydrothermal synthesis and characterisation of crystalline Al-T complex. Effects of tartrate precursor and Al(III):tartrate mol ratio in the synthesis of Al-T complex were also investigated.

## MATERIALS AND METHODS

This study used lab-grade chemicals as received from the supplier, namely $Al(NO_3)_3.9H_2O$, *L*-tartaric acid, KNa-tartrate tetrahydrate, demineralised water, ethanol, and NaOH. Infrared spectrophotometer (IRSpirit-T Shimadzu), powder-XRD (PANalytical X'Pert3 Powder), DTA-TGA (Shimadzu Simultaneous TG/DTA–DTG-60), UV Vis DRS (Thermo Scientific Evolution 220), and SEM (Thermo Scientific INSPECT-S50) were used for identification and characterizations of the synthesized products.

Synthesis of Al-T was carried out in a 50 mL Teflon-lined stainless-steel autoclave using distilled water as solvent at pH 7 with Al(III):tartrate mol ratios of 1:2, 2:1, and 2:3. The hydrothermal reaction was set at 150 °C for 24 hours, based on our preliminary study. The tartrate precursors used were KNa-tartrate and *L*-tartaric acid. The detailed amount of chemicals in each reaction is presented in Table 1.

First, the aqueous solution of Al(III) nitrate and the tartrate precursors were mixed and stirred in a beaker glass for a few minutes. The solution was then adjusted to pH 7 by adding a dilute sodium hydroxide solution. Next, the homogeneous solution was transferred into a 50 mL Teflon-lined stainless-steel autoclave. After the autoclave was tightly closed, it was placed in an oven, in which the reaction was set up at 150 °C for 24 hours. Next, the oven was cooled down to room temperature with a reduction rate of 5 °C/hrs. The solution was filtered off using Whatman filter paper no 41. The precipitate obtained from each reaction series was rinsed with ethanol, followed by warm demineralised water several times to remove any remaining-unreacted precursors. The solid was then dried in an oven at 105 °C for 3 hrs and then saved in a desiccator equipped with silica gel beads for 2 days. The dry solid was finally weighed.

Table 1. Details of each reaction used in this work

| Code | Al(III):Tartrate Mol ratios | $Al(NO_3)_3.9H_2O$ (g) | *L*-tartaric acid (g) | KNa-tartrate (g) |
|---|---|---|---|---|
| Al-1A | 1:2 | 0.375 | 0.300 | - |
| Al-1B | | 0.375 | - | 0.564 |
| Al-2A | 2:1 | 0.750 | 0.150 | - |
| Al-2B | | 0.750 | - | 0.282 |
| Al-3A | 2:3 | 0.750 | 0.450 | - |
| Al-3B | | 0.750 | - | 0.846 |

The dry solids were then identified by IR spectroscopy and powder-XRD, followed by a characterization of UV Vis DRS, DTA-TGA, and SEM. Infrared spectroscopy analyses were performed using the ATR method at 4000-400 $cm^{-1}$. Powder XRD analyses were done using Cu-Kα radiation (1.541874 Å) at 2θ angle of 10º to 90º. UV-Vis DRS analysis was performed in absorbance mode at 200 to 1,100 nm with a measurement point of 2.00 nm. DTA-TGA was conducted at 25 to 600ºC with an increasing rate of 10ºC/minute. SEM imaging was performed using FEI at magnification of 25,000 times. All identification and characterization of the products were performed in Universitas Brawijaya facilities, except the UV Vis DRS analysis, which was performed in UIN Maliki Malang.

The degree of crystallinity (*Xc*), average crystallite size (*D*), and band gap energy ($E_g$) were also calculated [20]. The calculation of the crystallinity degree (*Xc*) is given in Eq. 1, in which $A_c$ is the area of crystalline peaks and $A_a$ is the area of amorphous peaks, whereas the calculation of the average crystallite size is given in Eq. 2 based on Scherrer formula, in which *D* is the crystallite size, *k* is the Scherrer factor (0.94), $\lambda$ is the X-ray wavelength that is used, $\beta$ is the full width at half maximum of the peak, and $\theta$ is the Bragg angle.

Calculation of the band gap energy, shown in Eq. 3, was based on the Tauc plot method from the DRS data, in which $\alpha$ is the absorption coefficient, *h* is the Planck's constant, *v* is the frequency of proton, $E_g$ is the bandgap energy, and *B* is a constant. The $\gamma$ factor is determined by the electron transition in nature, and it is equal to ½ and 2 for the direct and indirect transition, respectively [20].

$$X_C = \frac{A_C}{A_C + Aa} \quad (1)$$

$$D = \frac{k\lambda}{\beta \cos\theta} \quad (2)$$

$$(\alpha \cdot hv)^{1/\gamma} = B\left(hv - E_g\right) \quad (3)$$

## RESULTS AND DISCUSSION

### Hydrothermal Synthesis of Aluminium(III)-Tartrate

From a total of 6 reactions (with conditions of pH 7, heated at 150 °C for 24 hrs, and using water as solvent), a white crystalline solid (Figure 2) was only precipitated out from the 2:1 reaction series, namely the Al-2A (132 mg) and Al-2B (150 mg). Other reactions result in a colourless solution with no precipitation. It indicates that the mol ratio plays a key role in the precipitation of the Al-T complex. This result was unprecedented since the 2:1 mol ratio is not stoichiometrically in line with the charge balance between $Al^{+3}$ and $(tartrate)^{-2}$. The excess amount of Al(III) is proposed to direct the reaction into the right side of the complexation equilibrium.

The yield obtained from the Al-2B reaction is higher than that of the Al-2A, suggesting that different tartrate precursors affect the Al-T complex's crystallisation. Particularly, the use of KNa-tartrate gives a higher yield than that of the *L*-tartaric acid, which is probably due to higher ionic tartrate species availability in the solution. In an aqueous solution, the weak tartaric acid has a lower probability of producing the anionic species than the tartrate salt. Thus, the complexation reaction between Al(III) and tartrate anions will likely to be occurred in the KNa-tartrate solution. It is noticed that this study limits the reaction that uses conditions of pH 7, 150 °C for 24 hrs, and water as solvent. Therefore, reactions that use other mol ratios may still be able to produce precipitated products if different reaction conditions were applied, for example, if the pH was changed into basic pH or the reaction used other solvent mixture, etc.

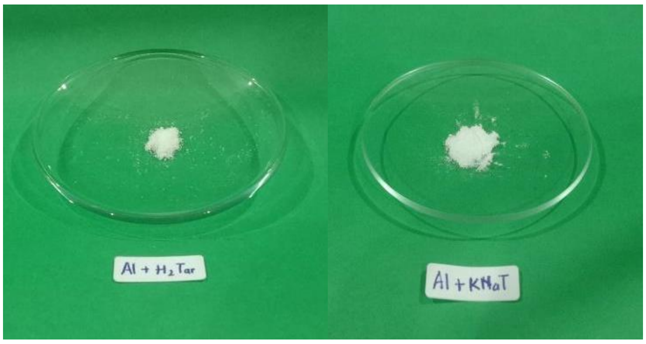

**Figure 2.** White solid of Al-T obtained from Al-2A (left) and Al-2B (right) reactions

### Characterization of Aluminium(III)-Tartrate Complex

ATR-IR was done to determine the functional groups within the product and to confirm the formation of Al-T complex. Infrared spectra of the products from the Al-2A and Al-2B reactions (Figure 3) were also compared with that of the precursors ($Al(NO_3)_3.9H_2O$, KNa-tartrate, and *L*-tartaric acid) to identify any changes in the infrared spectra that occurred due to metal-ligand bonds.

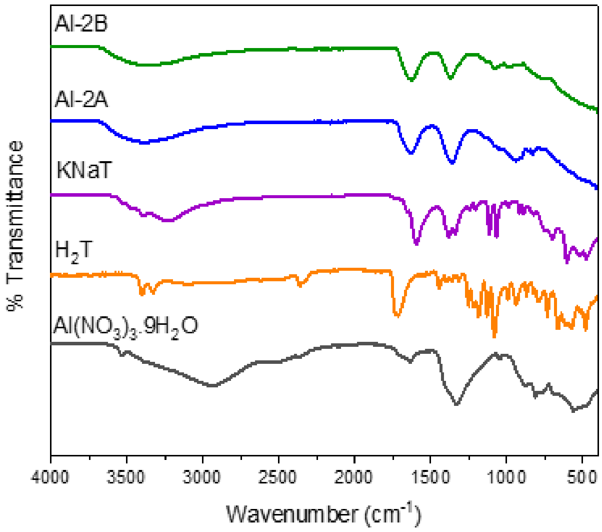

**Figure 3.** Infrared spectra of Al-2A and Al-2B compared to that of the precursors (KNa-tartrate, *L*-tartaric acid, and $Al(NO_3)_3.9H_2O$)

As shown in Figure 3, complexes from both Al-2A and Al-2B reactions show the presence of typical functional groups of tartrate ligands, namely the vibrations of the symmetric and asymmetric of the carboxylate, C–O, and C–OH groups. A change in pattern or shift in the absorption peak indicates the formation of a metal bond with the ligand, namely Al-O. In the Al-2A and Al-2B products, several peaks appear in 3377 and 3395 $cm^{-1}$ (O-H vibrations). The peaks in the areas of 1628 and 1631 $cm^{-1}$ indicate the presence of a C=O stretching group. In the Al-2B product, there is one peak in the area of 1370 $cm^{-1}$ and the Al-2A product in the area of 1357 $cm^{-1}$, which indicates the C=O stretching vibration and the O-C=O bending vibration, as well as the sharpness peaks of each product in the areas of 1079 and 1036 $cm^{-1}$ which indicate the C-O stretching group. It confirms that the precipitated product is Al-T complex.

The synthesised Al-T complexes were characterised by powder-XRD to determine the crystallinity degree and crystallite size. The powder diffraction patterns of Al-2A and Al-2B are presented in Figure 4. In general, both complexes show identical patterns but have different intensities. It suggests that both complexes have identical crystal systems. The crystallinity degrees of Al-2A and Al-2B are 44.23% and 59.87%, respectively, whereas the average crystallite sizes of Al-2A and Al-2B are 169.16 nm and 148.20 nm, respectively. These results show that each tartrate precursor may have different crystallization effects on the synthesized Al-T complex. Further analyses by DTA-TGA and UV-DRS were also performed to confirm this. Furthermore, when the diffraction pattern of both complexes is compared to previously reported Al-T by Lee *et al*. [15], they differ significantly. It is most likely due to the different precursors and synthesis conditions. Hence, although both procedures resulted in Al-T complexes, the crystal system of the compounds is proposed to be slightly different.

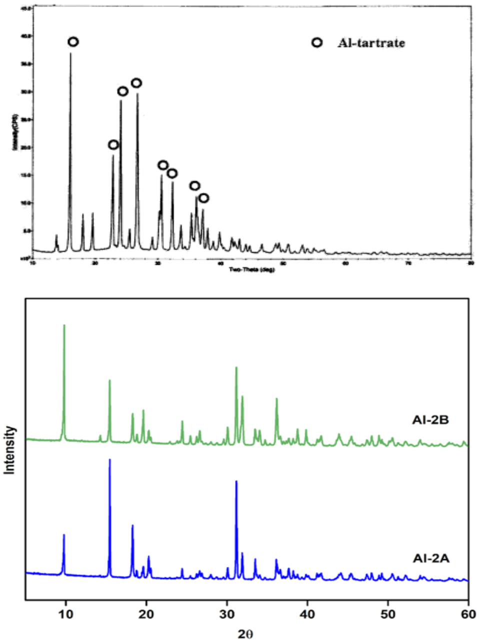

**Figure 4.** Powder diffraction patterns of the synthesized Al-T complexes obtained from the $H_2T$ (Al-2A) and KNaT (Al-2B), compared with that of the Al-T complex (top figure) reported by Lee [15].

UV-Vis DRS analysis was carried out not only to study the absorption profile and determine the band gap energy value of the synthesized Al-T complex but also to confirm whether both complexes are truly identical compounds. The absorption profile and its derivative to measure the band gap energy level are shown in Figure 5 and Figure 6, respectively.

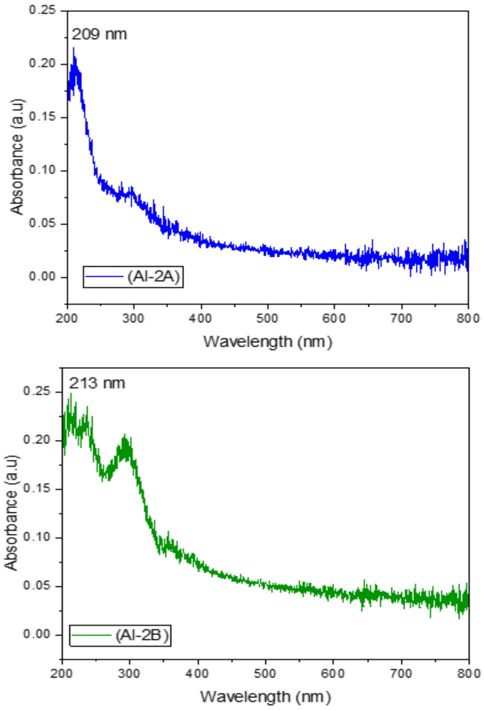

**Figure 5.** UV Vis absorption profile of the synthesized Al-T obtained from the Al-2A and Al-2B reactions

Both complexes absorb at nearly similar maximum wavelengths of 209 nm (Al-2A) and 213 nm (Al-2B), which correspond to the π→π* electronic transition of the tartrate ligand. Both complexes display nearly identical profiles, except around 300 nm, which is probably due to the presence of ionic impurities or crystal defects. The ionic impurities can also contribute through the electronic transition of n→π* or charge transfer from the alkali ions ($K^+$, $Na^+$) in the crystal packing of the Al-T, thus altering the electronic environment around the aluminium centre.

Moreover, the band gap energy levels produced by Al-2A and Al-2B are also the same, around 5.0 eV (Figure 6). This means that the Al-2A and Al-2B need a high energy to be activated as a photocatalyst, which is higher than the Al-terephthalate complex (3.54 eV) previously synthesized by Zokaee *et al* (2022) [21].

Furthermore, DTA-TGA characterization was carried out to determine the thermal stability profile of the complexes. Hence, the decomposition temperature of the compound can be observed. The TGA curve shows the decomposed mass, while the DTA curve shows the phase changes that occur during the decomposition of Al-T (Figure 7). Overall, both complexes have different thermogram profiles, which indicate that the Al-2A and Al-2B have different thermal stability and have different chemical formulas.

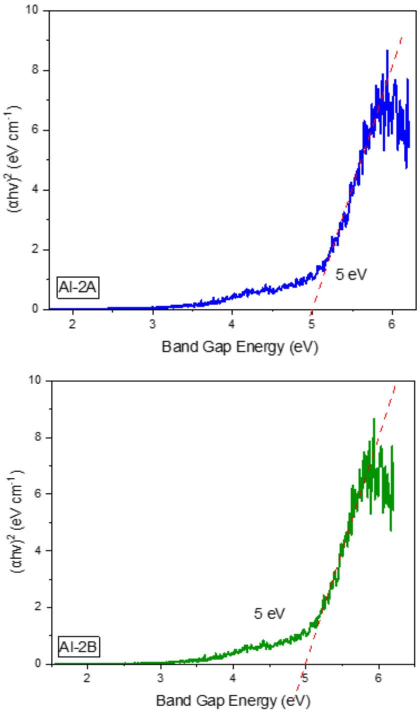

**Figure 6.** Band gap energy of the synthesized Al(III)- tartrate obtained from the Al-2A and Al-2B reactions

The early stage of decomposition of the Al-2B (room temperature to 150 C) occurred at a lower temperature than that of the Al-2A. It can be associated with the evaporation of water vapour adsorbed on the surface of Al-T and water molecules that are present in the crystal lattice. Surprisingly, the second decomposition stage of Al-2B occurred at a much higher temperature. This stage probably corresponds to the decomposition of the organic group of the tartrate ligand, including the possible breaking of the coordination bond between Al$^{3+}$ and the carboxylate or hydroxyl groups.

Characterization by SEM was performed to assess the surface morphology of the synthesized Al-T complex. Surprisingly, although the thermogram of both complexes shows significant differences, Al-2A and Al-2B exhibit considerably identical surface morphology of block-shaped crystalline particles (Figure 7). When compared to Lee’s work published in 2011, the synthesized Al-T has a more uniform crystal. Along with the powder XRD data, this work has produced a crystalline Al-T complex with different crystal structures.

For future work, a slow, controlled decrease in temperature during the cooling down of the reaction can be applied to increase the probability of producing bigger and better crystals.

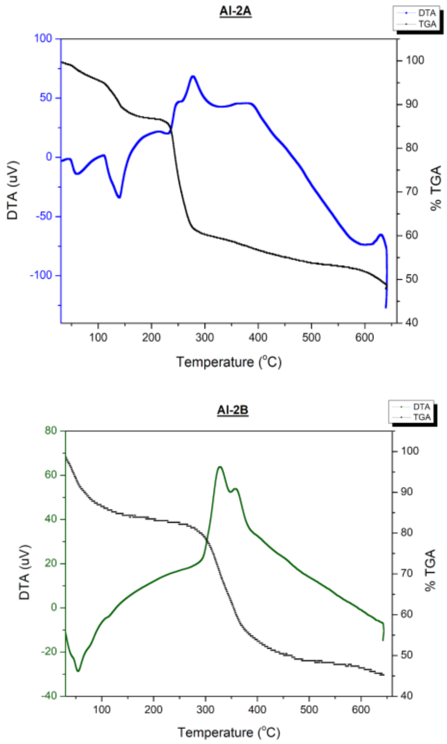

Figure 7. DTA (blue or green lines) and TGA (black lines) thermograms of the synthesized Al-T complex

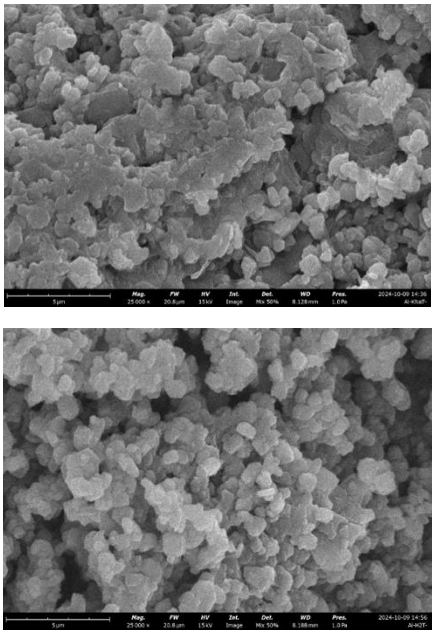

**Figure 8.** Surface morphology of the synthesized Al-T complexes from the Al-2A (top) and Al-2B (bottom) in 25,000x magnification

## CONCLUSION

Crystalline aluminium(III)-tartrate complexes were successfully obtained by hydrothermal method. Mol ratio affects the precipitation of the Al-T complex, in which only a mol ratio of 2:1 produces precipitate (white solid). Different tartrate precursors led to different yields. A higher yield was obtained from the KNa-tartrate than the $H_2$-tartrate precursor due to higher ionic tartrate species availability in the solution. Although both tartrate precursors resulted in identical block-shaped crystalline Al-T complex, each complex shows slightly different characteristics because of the different nature of the precursor. The Al-T complexes have the same band gap energy of 5.0 eV, have crystallinity degrees of 44.23% (Al-2A) and 59.87% (Al-2B), and have average crystallite sizes of 169.16 nm (Al-2A) and 148.20 nm (Al-2B).

## ACKNOWLEDGEMENTS

This work was funded through the Penelitian Dana Internal - Faculty of Mathematics and Natural Sciences, Universitas Brawijaya 2025 (Contract No 2612.6/UN01.F09/PN/2024). All authors acknowledge the Department of Chemistry and the Integrated Research Laboratory (LRT) in Universitas Brawijaya, Indonesia, for lab facilities and any support given.

## REFERENCES

[1] Jafar, N., Nurhawaisyah, S. R., Widodo, S., Chalik, C. A., & Wakila, M. H. (2023). Mineralogical Study of Bauxite of Kenco Area, Landak District, West Kalimantan Province, Indonesia. *IOP Conference Series: Earth and Environmental Science*, *1134*(1), 012025. https://doi.org/10.1088/1755-1315/1134/1/012025

[2] Kementerian ESDM Indonesia. (2020). Booklet Tambang Bauksit 2020. https://www.esdm.go.id/id/booklet/booklet-tambang-bauksit-2020. Retrieved December 27, 2024.

[3] Syarwani, A. & Prananto, Y. P. (2023). Literature Study on the Screening of Al-MOFs Porous Material for Dimethyl Ether (DME) Gas Purification. *Jurnal Integrasi Proses*, *12*(2), 55-65. https://dx.doi.org/10.36055/jip.v12i2.17485

[4] Joshi, J. N., Moran, C. M., Feininger, H. P., Dow, J. M., & Walton, K. S. (2019). Household Aluminum Products as Insoluble Precursors for Directed Growth of Metal–Organic Frameworks. *Crystal Growth & Design*, 19(9), 5097–5104.

[5] Ding, M., Cai, X., & Jiang, H. L. (2019). Improving MOF Stability: Approaches and Applications. *Chemical Science*, *10*(44), 10209-10230. DOI: 10.1039/C9SC03916C

[6] Samanidou, V. F., & Deliyannni, E. A. (2020). Metal Organic Frameworks: Synthesis and Application. *Molecules*, *25, 960*, 1. https://doi.org/10.3390/molecules25040960

[7] Yusuf, V. F., Malek, N. I., & Kailasa, S. K. (2022). Review on Metal–Organic Framework Classification, Synthetic Approaches, and Influencing Factors: Applications in Energy, Drug Delivery, and Wastewater Treatment. *ACS Omega*, *7*(49), 44507–44531. https://doi.org/10.1021/acsomega.2c05310

[8] Majumder, M., Choudhary, R. B., Thakur, A. K., Khodayari, A., Amiri, M., Boukherroub, R., & Szunerits, S. (2020). Aluminum based Metal-Organic Framework Integrated with Reduced Graphene Oxide for Improved Supercapacitive Performance. *Electrochimica Acta*, *353*, 136609. https://doi.org/10.1016/j.electacta.2020.136609

[9] Bansal, P., Mishra, D., Vijayakumar, A., & Chatterjee, S. (2023). Aluminium Terephthalate (Al-BDC) based Metal Organic Framework Decorated Carboxymethylated Filter Cloth For Defluoridation Application. *Journal of Environmental Chemical Engineering*, *11*(3), 110233. https://doi.org/10.1016/j.jece.2023.110233.

[10] Raju, U., Warkar, S. G., & Kumar, A. (2017). Green Synthesis of Multi Metal-Citrate Complexes and Their Characterization. *Journal of Molecular Structure*, *1133*, 90–94. https://doi.org/10.1016/j.molstruc.2016.11.084

[11] Horcajada, P., Gref, R., Baati, T., Allan, P. K., Maurin, G., Couvreur, P., Férey, G., Morris, R. E., & Serre, C. (2012). Metal–Organic Frameworks in Biomedicine. *Chemical Reviews*, *112*(2), 1232–1268. https://doi.org/10.1021/cr200256v

[12] Liu, J., Chen, L., Cui, H., Zhang, J., Zhang, L., & Su, C.-Y. (2014). Applications of Metal–Organic Frameworks in Heterogeneous Supramolecular Catalysis. *Chemical Society Reviews*, *43*(16),

6011–6061. https://doi.org/10.1039/C4CS00094C

[13] Cepeda, J., Pérez-Yáñez, S., Beobide, G., Castillo, O., Goikolea, E., Aguesse, F., Garrido, L., Luque, A., & Wright, P. A. (2016). Scandium/Alkaline Metal–Organic Frameworks: Adsorptive Properties and Ionic Conductivity. *Chemistry of Materials*, *28*(8), 2519–2528. https://doi.org/10.1021/acs.chemmater.5b03458

[14] Fujie, K., Ikeda, R., Otsubo, K., Yamada, T., & Kitagawa, H. (2015). Lithium Ion Diffusion in a Metal–Organic Framework Mediated by an Ionic Liquid. *Chemistry of Materials*, *27*(21), 7355–7361. https://doi.org/10.1021/acs.chemmater.5b02986

[15] Lee, H.-Y. (2011). A Study on the Synthesis of Aluminum Tartrate from Aluminum Chloride Solutions. *Resources Recycling*. *20*(2), 54-59. https://doi.org/10.7844/kirr.2011.20.2.054

[16] Greenstein, G. R. (2007). The Merck index: An Encyclopedia of Chemicals, Drugs, and Biologicals. *Reference Reviews*, *21*(6), 40-40. https://doi.org/10.1108/09504120710775534

[17] Desroches, S., Daydé, S., & Berthon, G. (2000). Aluminum Speciation Studies in Biological Fluids. *Journal of Inorganic Biochemistry*, 81(4), 301–312. https://doi.org/10.1016/s0162-0134(00)00072-6

[18] Khunur, M. M., & Prananto, Y. P. (2018). Synthesis and Structure of 2D Cobalt(II)-tartrate Hydrate Coordination Polymers Crystallised from Aqueous Solution. *Bulletin of Chemical Reaction, Engineering, & Catalysis*, *13*(2), 213–219. https://doi.org/10.9767/bcrec.13.2.1342.213-219

[19] Prananto, Y. P., Wibisono, R. D., Fadhilah, S. G., Tjahjanto, R., Darjito, & Salsabila, F. L. (2022). Crystallization of Mn(II) and Cd(II) Complexes in A Water-Methanol System: Tartrate vs Nicotinamide Ligand Selectivity. *Acta Chimica Asiana*, *5*(1), 166–172. https://doi.org/10.29303/aca.v5i1.114

[20] Rafika, A. H., Khunur, M. M., Tjahjanto, R. T. & Prananto, Y. P. (2022). Effect of Drying Temperature and Drying Time On The Crystallinity Degree of Zn(II)-tartrate Complex. *Kuwait Journal of Chemistry*, *50*(4), 596–601. https://doi.org/10.1016/j.kjs.2023.03.007

[21] Zokaee, Z., Mahmoodi, N. M., Rahimpour, M. R., & Shariati, A. (2022). Synthesis of visible light activated metal-organic framework coated on titania nanocomposite (MIL-53(Al)@$TiO_2$) and dye photodegradation. *Journal of Solid State Chemistry*, *307*, 122747. https://doi.org/10.1016/j.jssc.2021.122747